J Electr Eng Technol Vol. 9, No. 6: 1935-1943, 2014
http://dx.doi.org/10.5370/JEET.2014.9.6.1935

ISSN(Print) 1975-0102
ISSN(Online) 2093-7423

Analysis of Harmonic Currents Propagation on the Self-Excited Induction Generator with Nonlinear Loads

Refdinal Nazir†

Abstract – In recent years, the induction machines are increasingly being used as self-excited induction generators (SEIG). This generator is especially widely employed for small-scale power plants driven by renewable energy sources. The application of power electronic components in the induction generator control (IGC) and the loading of SEIG using nonlinear loads will generate harmonic currents. This paper analyzes the propogation of harmonic currents on the SEIG with nonlinear loads. Transfer function method in the frequency domain is used to calculate the gain and phase angle of each harmonic current component which are generated by a nonlinear loads. Through the superposition approach, this method has also been used to analyze the propagation of harmonic currents from nonlinear load to the stator windings. The simulation for the propagation of harmonic currents for a 4 pole, 1.5 kW, 50Hz, 3.5A, Y-connected, rotor-cage SEIG with energy-saving lamps, have provided results almost the same with the experiment. It can prove that the validity of the proposed models and methods. The study results showed that the propagation of harmonic currents on the stator windings rejects high order harmonics and attenuates low order harmonics, consequently THD_I diminish significantly on the stator windings.

Keywords: Self-Excited Induction Generator (SEIG), Transfer fuction, Nonlinear loads, Harmonics, Total Harmonic Distortion (THD).

1. Introduction

Nowaday, the induction generator is more popular used for small-scale power plants driven by renewable energy sources, including: wind, mini/microhydro, tidal wave, biomass, biogas, etc.[1]. The popularity of induction generator mainly is due to a number of advantages compared to conventional generators, such as: low cost, high reliability, rugged construction, maintenance and operational simplicity, self-protection against faults and overload, not needed dc supply for excitation, etc. [1, 2]. The application of induction generators in commercial biogas driven power has been successfully analyzed [1]. Some experts have successfully designed the induction generator control (IGC), consequently this generator can be used commercially on a micro hydro power plant [3-5]. In the meantime, the minimum excitation capacitor connected auxiliary windings of a single phase Self-Excited Induction Generator (SEIG) have been successfully calculated for suitable for stanby power system [6].

However, the operation of the induction machine as a generator requires reactive power, which is supplied either from the grid or compensation capacitors. It will leads the generator to produce power with low power factor. In addition, the utilization of power electronics components on the IGC and/or non-linear loads will generate harmonics current and voltage on the generator output. The harmonics distortion can give the effect of a decrease in efficiency, heating and reducing the lifetime of the machine [7].

Currently, the performance analysis of SEIG was more focused supplying linear loads. The publications about the study of SEIG with nonlinear loads is little relatively. Only in literature [8], the behaviour of SEIG with nonlinear loads has been analyzed specifically using the dynamic model. In this paper, the propagation of harmonic currents on SEIG with nonlinear load is analyzed using the steady state model. Again, the superposition approach is employed to analyze the effects of each source voltage generated by the generator and source of harmonic currents generated by the nonlinear load. Transfer function in the frequency domain is used to calculate the current gain of each harmonic component generated by nonlinear load. Simulation and experimental results are compared to test the validity of the model and method used.

This paper is organized into 5 sections. Modeling and analysis of SEIG with non-linear load is discussed in section 2. The experimental set-up are explained in section 3. The section 4 discusses the results and its analysis. Conclusions are presented in section 5.

2. The Steady State Analysis of SEIG with Nonlinear Loads

The configuration of single line diagram of the SEIG

† Corresponding Author: Dept. of Electrical Engineering, Andalas University, Indonesia. (refdinalnazir@yahoo.co.id)
Received: February 4, 2014; Accepted: May 19, 2014

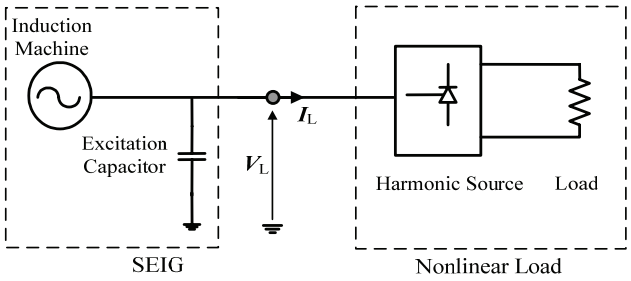

Fig. 1. Cofiguration of SEIG with nonlinear load

with nonlinear loads is shown in Fig. 1. The SEIG is constructed by an induction machine and an excitation capacitor, and is connected to nonlinear loads. In this case, nonlinear load is load equipped with electronic device, such as: uninterruptable power supply (UPS), adjustable speed drives (ASD), variable frequency drive (VFD), saving-energy lamps, etc. SEIG, either as generator set or micro hydro generator, supply nonlinear loads that generated harmonic currents.

2.1 The modelling and analysis of SEIG with nonlinear loads

In the previous study, the per-phase equivalent circuit of SEIG has been employed permanently to analyze the steady state performance of SEIG with linear loads [9-11]. The per-phase equivalent circuit of SEIG with necglecting core loss is shown in Fig. 2. Where, R_s, X_s, R_r, X_r, and X_m are the stator resistance, stator leakage rectance, rotor resistance, rotor leakage rectance, and magnetizing reactance respectively. Furthermore, R_L, X_L, and X_c represent the load resistance, load reactance, and excitation capacitor reactance. $\sigma = a\text{-}b$, is slip, where a and b represent per unit (p.u.) frequency and rotor speed respectively. The equivalent circuit of SEIG with nonlinear loads can be obtained from the modification of this equivalent circuit. In this modification, the branch of linear load (R_L/a dan X_L) in Fig. 2 is changed with nonlinear load model.

The equivalent circuit simplified of SEIG with nonlinear load is shown in Fig. 3. In this circuit, the amplitude and frequency of the load voltage V_L is assumed a constant at the nominal rating. Consequently, the value of a in this equivalent circuit is always one. As shown in Fig. 3, the nonlinear load is modeled as harmonic current sources, I_1, I_2,...I_h , where h (2^{nd}, 3^{rd}, 5^{th}, 7^{th},....) is known the order of the harmonics. While, SEIG is formed as the single voltage source, V_{ig}, that connected in series an internal impedance, Z_{ig}. The voltage source of SEIG is the open circuit voltage across the load terminals 1-2 (see Fig. 2), $V_{ig} = V_L(OC)$. Whereas, the internal impedance of SEIG is the impedance across the load terminal 1-2 in Fig. 2.

The superposition approach is used to analyze the propagation of harmonic currents. In this approach, each source is considered to evaluate the current through the

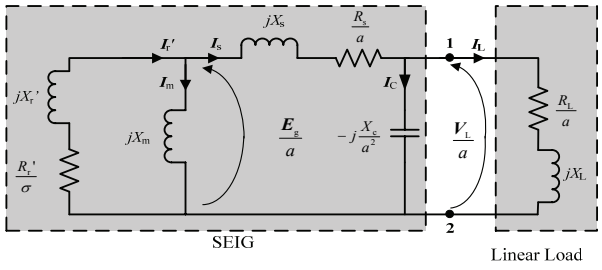

Fig. 2. Equivalent circuit per-phase of SEIG under linear load with neglecting core loss

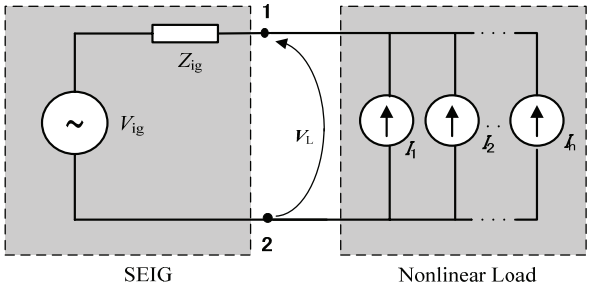

Fig. 3. Equivalent circuit simplified of SEIG with nonlinear loads

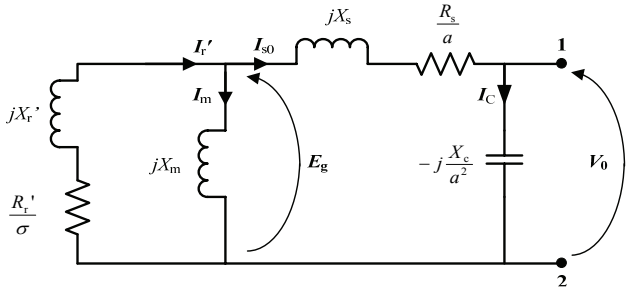

Fig. 4. Equivalent circuit of SEIG for voltage sources response

stator windings seperately.

2.1.1 Voltage source response

In voltage source response, the analysis is conducted by replacing all current sources with an open circuit. This situation can occur in SEIG under no-load condition. The equivalent circuit of SEIG under no-load condition is shown in Fig. 4. In this conditions, the stator current I_{s0} is equal with the excitation current I_C.

Due to saturation effects, the value of X_m is influenced by the magnetizing current I_m, which can be expressed as follows,

$$X_m(I_m) = \sum_{i,j=0}^{n} \alpha_i I_m^j \qquad (1)$$

There is constant value of α_i resolved from the polynomial curve fitting using saturation test results and n is the degree of polynomial equation.

2.1.2 Current Sources Response

For harmonic current sources response, the analysis is performed considering one current source I_h. While, the other current sources and voltage source are replaced respectively with an open circuit and and internal impedance of SEIG. The equivalent circuit for one harmonic current source response is given in Fig. 5. This circuit is expressed in the domain *s* in order to simplify the analysis. In this condition, the inductive reactances are expressed by *sL* and the capacitive reactances are presented as 1/*sC*.

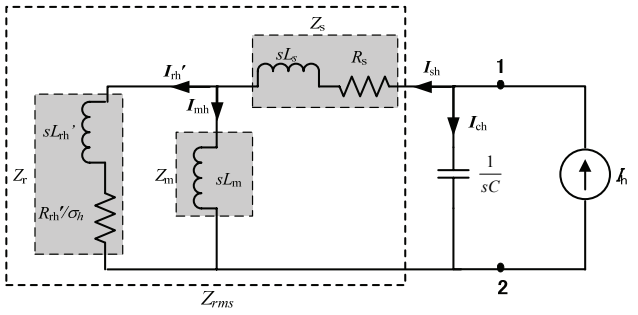

Fig. 5. SEIG equivalent circuit for current source response

The harmonics distortion on SEIG will effect on its parameter and variable values. The stator parameters (R_s and L_s) have a constant value, while the value of rotor parameters (R_r' and L_r') depend on the order of harmonics, due to skin effect [12, 13]. Meanwhile, the amount of total rms of magnetizing current I_m(rms) can be calculated as follow [14],

$$I_m(rms) = \sqrt{I_{m1}^2(rms) + I_{m2}^2(rms) + I_{m3}^2(rms) ... + I_{mh}^2(rms)} \tag{2}$$

Where, I_{mh} is the rms value of magnetising current for h^{th} order harmonic. In addition, the effect of harmonics on the slip is expressed by the following Eq. [2]:

$$\sigma_h = \frac{h\omega_1 - \omega_r}{h\omega_1} \tag{3}$$

where σ_h is the slip at harmonic order *h*, and ω_1 & ω_r are fundamental frequency and rotor speed respectively.

To referring Fig. 4, the rotor impedance $Z_{rm} = \frac{R'_{rh}}{\sigma_h} + sL'_{rh}$ is connected parallel to the magnetization impedance, $Z_m = sL_m$, hence the total impedance for these branches are:

$$Z_{rm} = \frac{R'_{rh}}{\sigma_h} + sL'_{rh} // sL_m = \frac{sL_m\left(\frac{R'_{rh}}{\sigma_h} + sL'_{rh}\right)}{\frac{R'_r}{\sigma_h} + sL_m + sL'_{rh}} \tag{4}$$

The impedance Z_{rm} is connected in series with the stator impedance, $Z_s = R_s + sL_s$, so the total impedance at this branch is:

$$Z_{rms} = \frac{sL_m\left(\frac{R'_{rh}}{\sigma_h} + sL'_{rh}\right)}{\frac{R'_r}{\sigma_h} + sL_m + sL'_{rh}} + R_s + sL_s \tag{5}$$

If $\frac{R'_r}{\sigma_h} = R'_{r\sigma}$ and $(L_m + L'_{rh}) = L_{mr}$, then Eq. (5) can be modified as:

$$Z_{rms} = \frac{(sL_m R'_{r\sigma}) + (s^2 L_m L'_{rh})}{R'_{r\sigma} + sL_{mr}} + R_s + sL_s \tag{6}$$

or

$$Z_{rms} = \frac{(sL_m R'_{r\sigma}) + (s^2 L_m L'_r) + (sR'_{r\sigma} L_s) + (sR_s L_{mr}) + (s^2 L_s L_{mr}) + (R'_{r\sigma} R_s)}{R'_{r\sigma} + sL_{mr}} \tag{7}$$

The equivalent circuit in Fig. 5 can be simplified to Fig. 6.

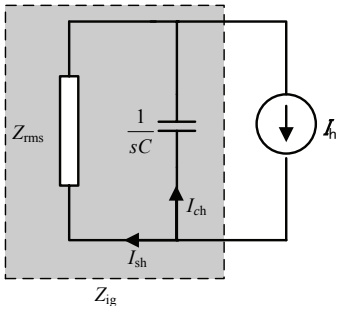

Fig. 6. Simplified representation of the equivalent circuit of Fig. 5.

From the equivalent circuit of Fig. 6, the transfer function *T*(s) as a current gain between the load and stator currents can be written as,

$$T(s) = \frac{I_{sh}}{I_h} = \frac{\frac{1}{sC}}{\frac{1}{sC} + \frac{(sL_m R'_{r\sigma}) + (s^2 L_m L'_r) + (sR'_{r\sigma} L_s) + (sR_s L_{mr}) + (s^2 L_s L_{mr}) + (R'_{r\sigma} R_s)}{R'_{r\sigma} + sL_{mr}}} \tag{8}$$

or

$$T(s) = \frac{R'_{r\sigma} + sL_{mr}}{s^3(L_s L_{mr} C + L_m L'_r C) + s^2(R'_{r\sigma} L_m C + R'_{r\sigma} L_s C + R_s L_{mr} C) + s(R'_{r\sigma} R_s C + L_{mr}) + R'_{r\sigma}} \tag{9}$$

In the frequency domain $s = j\omega$, the transfer function (Eq. 9) can be expressed as:

$$T(j\omega)=\frac{R'_{r\sigma}+j\omega L_{mr}}{(j\omega)^3\left(L_sL_{mr}C+L_mL'_rC\right)+(j\omega)^2\begin{pmatrix}R'_{r\sigma}L_mC+R'_{r\sigma}L_sC\\+R_sL_{mr}C\end{pmatrix}+j\omega\left(R'_{r\sigma}R_sC+L_{mr}\right)+R'_{r\sigma}} \quad (10)$$

or

$$T(j\omega)=\frac{R'_{r\sigma}+j\omega L_{mr}}{R'_{r\sigma}-\omega^2\left(R'_{r\sigma}L_mC+R'_{r\sigma}L_sC+R_sL_{mr}C\right)+j\left\{\omega\left(R'_{r\sigma}R_sC+L_{mr}\right)-\omega^3\left(L_sL_{mr}C+L_mL'_rC\right)\right\}} \quad (11)$$

The magnitude of the transfer function can be solved from the following equation:

$$\left|T(j\omega)\right|=\frac{\sqrt{R'^2_{r\sigma}+(\omega L_{mr})^2}}{\sqrt{\left\{R'_{r\sigma}-\omega^2\left(R'_{r\sigma}L_mC+R'_{r\sigma}L_sC+R_sL_{mr}C\right)\right\}^2+\left\{\omega\left(R'_{r\sigma}R_sC+L_{mr}\right)-\omega^3\left(L_sL_{mr}C+L_mL'_rC\right)\right\}^2}} \quad (12)$$

where $\omega=h\omega_1$, ω_1 is the fundamental frequency of generator.

While, the phase angle of the transfer function can be calculated as:

$$\theta=\text{Arc tan}\left(\frac{\omega L_{mr}}{R'_{r\sigma}}\right)-\text{Arc tan}\left\{\frac{\omega\left(R'_{r\sigma}R_sC+L_{mr}\right)-\omega^3\left(L_sL_{mr}C+L_mL'_rC\right)}{R'_{r\sigma}-\omega^2\left(R'_{r\sigma}L_mC+R'_{r\sigma}L_sC+R_sL_{mr}C\right)}\right\} \quad (13)$$

To re-referring Fig. 5, the current I_{sh} propagate to the magnetizing inductance L_m can be determined as:

$$\frac{I_{mh}}{I_{sh}}=\frac{\frac{R'_{rh}}{\sigma_h}+j\omega L'_{rh}}{\frac{R'_{rh}}{\sigma_h}+j\omega\left(L_m+L'_{rh}\right)} \quad (14)$$

or

$$\frac{I_{mh}}{I_{sh}}=\frac{R'_{r\sigma}+j\omega L'_{rh}}{R'_{r\sigma}+j\omega L_{mr}} \quad (15)$$

2.2 Induction machine parameter test

In this study, 4 pole ; 380-420V, 1.5 kW, 50 Hz; 3.5A; Y-connection; rotor-cage induction machine is used. The DC test, no-load test and blocked-rotor test are conducted to determine the machine parameters. In addition, saturation test and testing the influence of harmonics on the rotor resistance and inductance are also performed. Through the parameter test is obtained $R_s = 4.70\ \Omega$ and $X_s = 5.07\ \Omega$.

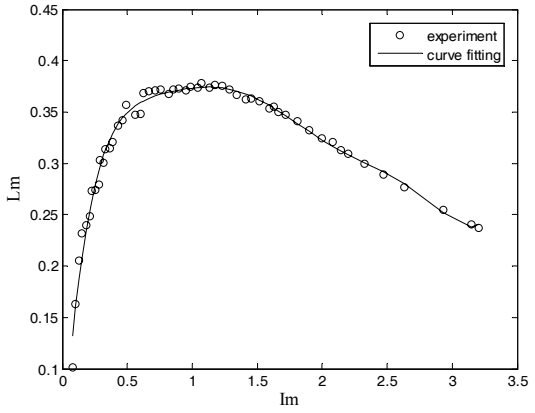

Fig. 7. Variation of magnetizing inductance L_m against magnetizing current I_m

The variation of the magnetizing inductance L_m against the magnetizing current I_m can be completed from saturation test results, as shown in Fig. 7. The procedure test is explained in Appendix. By using the curve fitting, this relationship can be presented in 7th order polynomial equation, as:

$$L_m = 0.0196I_m^7-0.2414I_m^6+1.2042I_m^5-3.1400I_m^4+4.6093I_m^3-3.8713I_m^2+1.7789I_m+0.0139 \quad (16)$$

The influence of harmonics on the rotor resistance, R_{rh}', and inductance, L_{rh}', are measured through blocked-rotor test. Generally, the induction machines is operated at low slip (2-4%), therefore the frequency of rotor currents is in the range from 1 to 2 Hz [15]. During blocked-rotor test, slip is one, hence the stator frequency is equal with the rotor frequency. In this test, the fundamental rotor frequency is taken 5 Hz, and 10 Hz, 15 Hz, 20 Hz,... are used as harmonics frequency in 1st, 2nd, 3rd, 4th,... order. The variation of the rotor resistance, R_{rh}', and inductance, X_{rh}' against the harmonics order, h, are shown in Figs. 8 and Fig. 9 respectively. By using the curve fitting, this relationship can be presented in 6th order polynomial equation, as follow:

$$R_{rh}' = \{-0.0001h^6+0.0860h^5-4.5835h^4+90.9904h^3-838.7662h^2+4598.8297h+25718.8306\}\times 10^{-4} \quad (17)$$

and

$$X_{rh}' = \{0.0394h^6-2.7571h^5+75.4347h^4-1014.3451h^3+6876.0846h^2-21304.3039h+66036.5027\}\times 10^{-4} \quad (18)$$

In the simulation, Eqs. 17 and 18 are used for harmonics number till 20th, and can be assumed a constant for harmonics number above 20th.

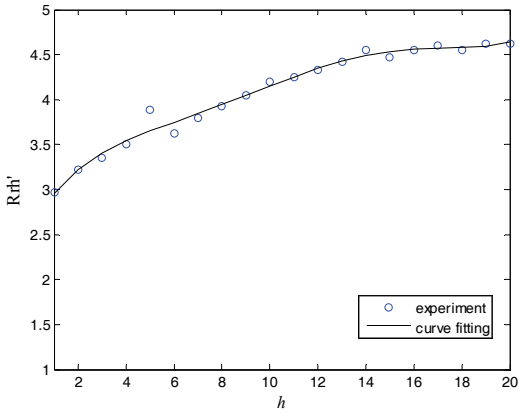

Fig. 8. Variation of rotor resistance R_{rh}' against h

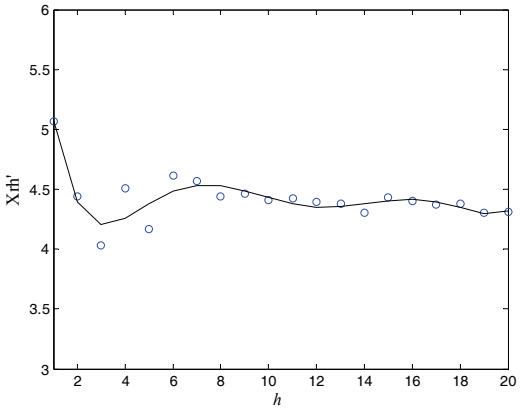

Fig. 9. Variation of rotor inductance X_{rh}' against h

2.3 Computer Simulation

The computer simulation is designed to solve the spectrum of transfer function and the propagation of harmonic currents on the stator windings. The design of computer program is developed from the flow chart in Fig. 10. The initial magnetizing current $|I_{m0}|$ is assumed similarly with the excitation current at no-load condition $|I_{c0}|$. L_{m0} is solved ploting $|I_{m0}|$ on the magnetising curve (see Fig. 5). In addition, ε is a small quantity ($\varepsilon = 10^{-6}$).

3. Experimental Set Up

In order to validate the results of the modeling and analysis, a series of experiment are performed in the laboratory. The experiment set up for the SEIG with nonlinear is shown by Fig. 11. In this test, a 3hp induction motor supplied by a frequency regulator is used as an activator of SEIG. The excitation capacitors used in this test is $3 \times 34\mu$F, which are connected in Y connection. The generator is burdened by nonlinear load, which is an energy-saving lamps of 1200 Watt. The harmonic measurements are performed using Power Analyzer type CA 8220 with data transfer to a PC/Laptop. The measurements were taken at two points of measurement,

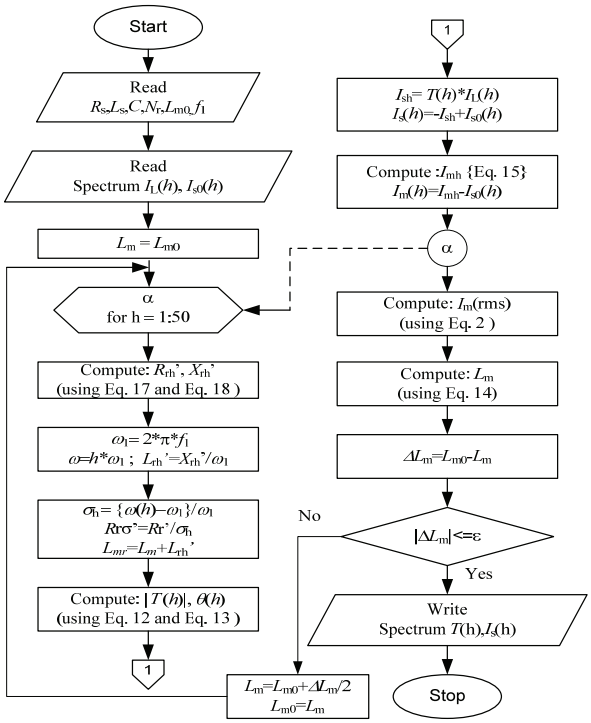

Fig. 10. Flow chart for computation of spectrum transfer function and stator current

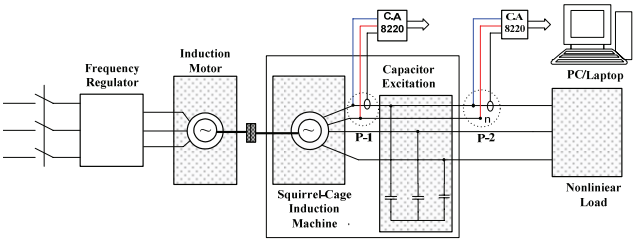

(a) Experiment circuit

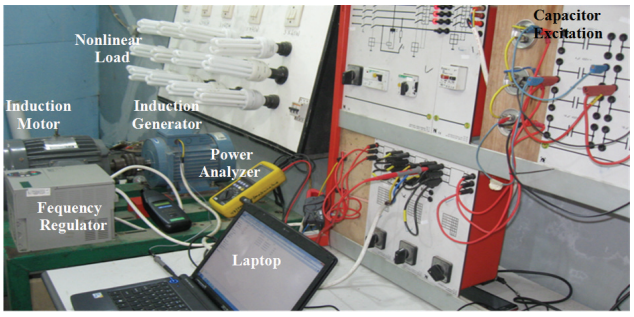

(b) photo

Fig. 11. Experiment set up for the proposed system

namely: on the load side (P-2) and on the stator windings side (P-1). During testing, both in the no-load condition and the nonlinear load condition, the fundamental frequency of terminal voltage generator is kept a 50 Hz constant by adjusting the speed rotor. The rotor speed for no-load condition is 1507 rpm, while rotor speed for load condition is 1539 rpm.

4. Results and Discussion

4.1 Simulation results of transfer function analysis

The transfer function analysis is employed to investigate the propagation of harmonic currents generated by nonlinear load to the stator windings of SEIG. In theory, the analysis of the transfer function has been carried out in section 2.1 (Eqs. 12 and Eq. 13). The simulation results for magnitude and phase angle of the transfer function are shown in Fig. 12. As shown in Fig. 12(a), the magnitue of transfer function has significantly its value for low order harmonics, and above order 20th harmonics are negligible. The phase angle of transfer function has always a positive value, and can be negligible for higher than order 20th (see Fig. 12(b)).

4.2 Experimental results of SEIG under no load

Fig. 13 shows the output of SEIG under no-load test. As shown in Fig. 13a, the stator current I_{s0} is leading against the output voltages V_0. At no-load condition, the stator windings is only flowed the current that generated by the excitation capacitor. In this condition, the generator has generated harmonic currents and voltages, with THD by 5.7% and 4.9% respectively (see Fig. 13(b)). The generated harmonics are relatively low and are the innate nature of SEIG.

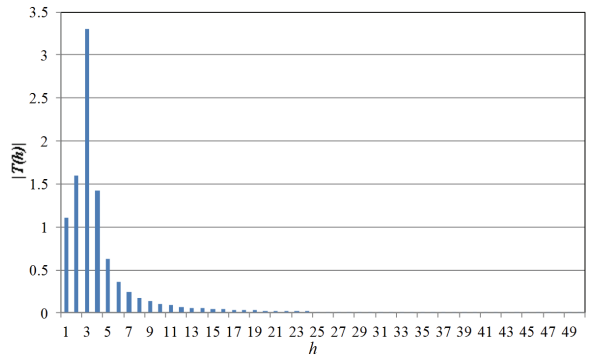

(a) Magnitude

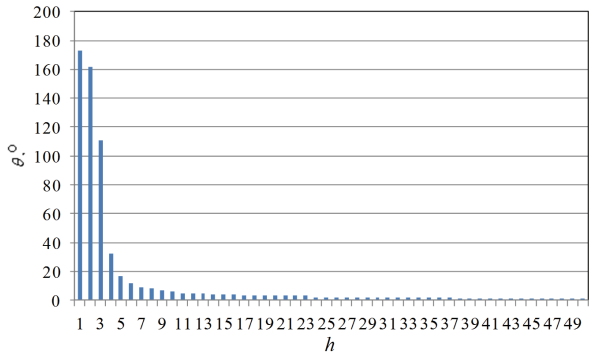

(b) Phase angle

Fig. 12. Simulation results for values of the transfer function

4.3 Experimental results for SEIG with nonlinear load

Fig. 14 shows the measurement results of the harmonic spectrum for current and voltage on the load side (P-2). As shown by Fig. 14(b), the component of harmonic currents spread from low to high order, with THD_I of 35.4%. This is obvious from results recording the waveform of load current (Fig. 14(a)), which showed a distorted badly from the ideal sinusoidal shape. Meanwhile the voltage waveform is slightly distorted, with THD_V only reached 9.5%.

The Spectrum of harmonic currents and voltages on the stator windings side (P-1) are shown by Fig. 15. As shown by this figure, the propagation of harmonic currents that generated by nonlinear load (P-2) on the stator winding

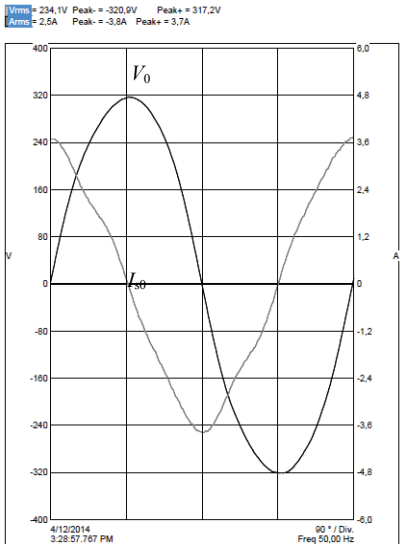

(a) Stator current and voltage ouput waveforms

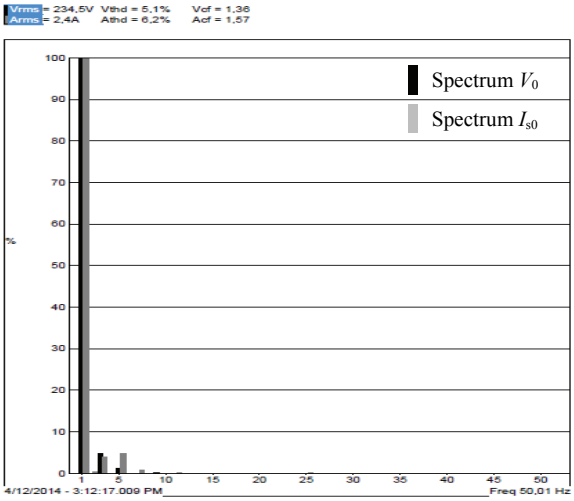

(b) Current and voltage harmonics spectrum

Fig. 13. The ouput of SEIG under no-load condition

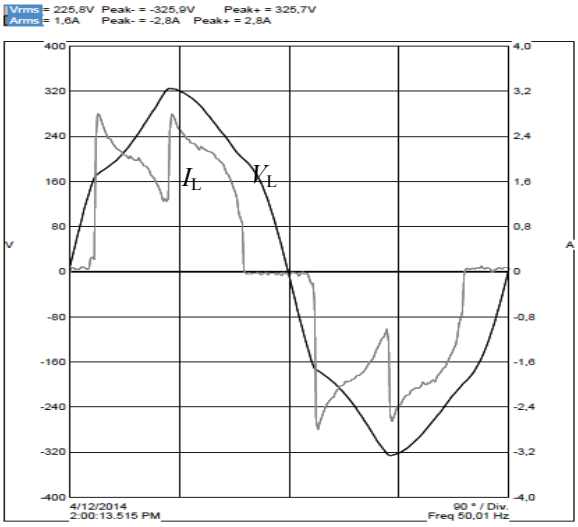

(a) Load current and voltage waveforms

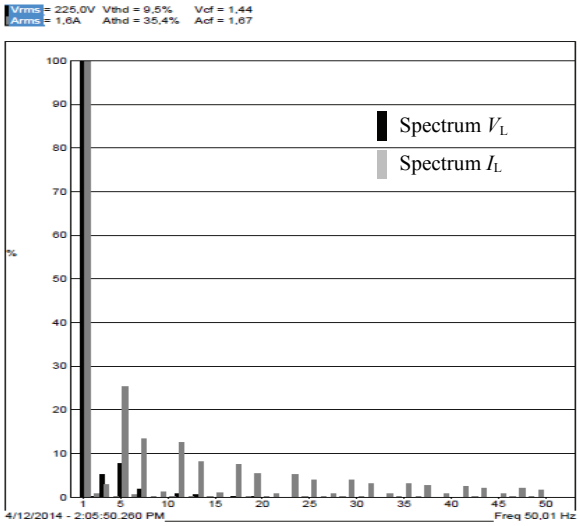

(b) Current and voltage load harmonics spectrum

Fig. 14. The measurement results on the load side (P-2)

have filtered significantly by SEIG, so that its THD_I is only 17.9%. In this case, the SEIG circuit has eliminated nearly all high order harmonic components. Whereas, harmonic current in order 5th, 3rd, and 7th are still emerging, but its amplitude has reduced.

4.4 Simulation results of SEIG with nonlinear load

The spectrum of harmonic currents on the stator windings of SEIG can be solved from the summation of all current sources and voltage source response. For the current sources response, the propagation of all harmonic currents generated by nonlinear loads on the stator windings are determined by multiplying each component of the transfer function spectrum (Fig. 12) and the load current spectrum (Fig. 14(b)). Meanwhile, the response of the voltage source is harmonic currents spectrum on the

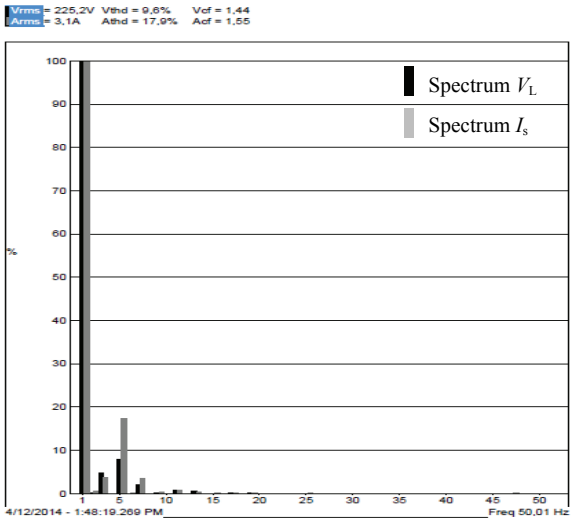

Fig. 15. Current and voltage stator harmonics spectrum on the stator side (P-1)

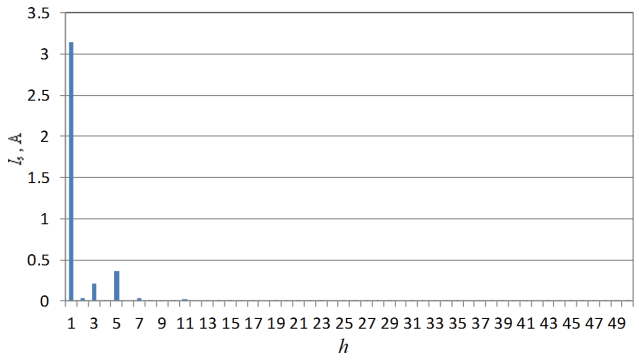

Fig. 16. Simulation results for spetrum harmonics of stator current I_s

stator windings of SEIG in the no-load condition (Fig. 13(b)). All above calculation have performed using computer program based the flow chart in Fig. 10. The simulation results of the spectrum for harmonic currents on the stator windings is shown in Fig. 16. As shown this figure, the component of harmonic currents that appear on the stator windings is only order 5th and 7th, while the component of higher order harmonics does not arise at all. THD_I of the stator current from simulation is 13.38 %.

4.5 Discussion

The simulation and experiment results have provided the same conclusion, that SEIG rejects or attenuates the propagation of harmonic currents from the load to the stator windings. As shown in Figs. 15 and Fig. 16, SEIG rejects almost all the high order component of hamornic currents on the stator windings, and attenuates the low order component.

On other hand, the current on the stator windings is the sum of the current of excitation capacitor and the load current containing harmonic components. In the stator

windings, the current component of excitation capacitor is greater than the current generated by nonlinear load. Consequentially, the contribution of the load current containing harmonic on the stator winding is small relatively, so THD_I is small too.

For loading SEIG with the energy-saving lamps of 1200 Watt, the propagation of harmonic currents reduced from THD_I of 35.4 % on the loads side to 17.9 % (experimental result) or 13.38 % (simulation result) on the stator windings side.

5. Conclusions

The transfer function method in frequency domain has been successfully used to calculate a current gain and its phase angle of each harmonic current component is generated by a nonlinear load. Through the superposition approach, this method has also been successfully used to analyze the propagation of harmonic currents generated by nonlinear load to the stator windings of SEIG.

The simulation and experiment have provided similar results. This shows that the models and methods used has adequate validity. Generally, The study results showed that the propagation harmonic currents created by loads on the stator widings of SEIG are rejected for high order components, and attenuated for lower order components. Consequently, the THD_I of stator current will be reduced significantly. In this study, the reduction percentage of harmonic current distortion on the stator windings reached 49.44% (experimental results) or 62.20% (simulatian results). It can be showed that SEIG has a friendly nature to the harmonics distortion generated by nonlinear loads.

Acknowledgements

Author would like thanks to Engineering Faculty, Andalas University for the financial support this work, through DIPA Funding (No. 032/PL/SPK/PNP/FT-Unand/ 2013).

References

[1] Li Wang and Ping-Yi Lin, Analysis of a Commercial Biogas Generation System Using a Gas Engine-Induction Generator Set, *IEEE Transactions on Energy Conversion,* Vol. 24, No. 1, pp. 230-239, March 2009.

[2] E. Muljadi, C.P. Butterfield, H. Romanowitz, and R. Yinger*, Self Excitation and Harmonics in Wind Power Generation*, National Renewable Energy Laboratory, November 2004.

[3] Bhim Singh and V. Rajagopal, "Battery Energy Storage Based Voltage and Frequency Controller for Isolated Pico Hydro Systems", Journal of Power Electronics, Vol. 9, No. 6, pp. 874-883, November 2009.

[4] Bhim Singh, S. S. Murthy and Sushma Gupta, "Analysis and Design of Electronic Load Controller for Self-Excited Induction Generators", IEEE Transactions on Energy Conversion, Vol. 21, No. 1, pp. 285-293, March, 2006.

[5] B. Singh, S.S. Murthy and S. Gupta, "Analysis and implementation an electronic load controller for a self-excited induction generator", IEE Proc-Gener. Transm. Distrib., Vol. 151, No. 1, pp. 51-60, January 2004.

[6] Cherl-Jin Kim and Kwan-Yong Lee, "A Study on the Modelling and Design of Single Phase Induction Generators", KIEE International Transaction on Electrical Machinery and Energy Convertion System, Vol. 5-B, No. 4, pp. 331-336, 2005.

[7] Hashem Oraee Mirzamani & Azim Lotfjou Chobari, "Study of Harmonics Effects on Performance of In-duction Motors", www.wseas.us/ elibrary/conferences/2005prague/papers/493.

[8] Samir Moulahoum and Nadir Kabache, "Behaviour Analysis of Self Excited Induction Generator F eeding Linear and No Linear Loads", Journal of Electrical Engineering & Technology, Vol. 8, No. 6, pp. 1371-1379, 2013.

[9] R. C. Bansal, "Three-Phase Self-Excited Induction Generator: An Overview", IEEE Transactions on Energy Convertion, Vol. 20 No. 2, pp. 292-299, June 2009.

[10] M. H. Haque, "A Novel Method of Evaluating Performance Characteristics of a Self-Excited Induction Generator", *IEEE Transactions on Energy Conversion*, Vol. 24, No. 2, pp. 358-365, June 2009.

[11] S.S. Murthy, O.P. Malik & A.K. Tandon, "Analyasis of Self-Excited Induction Generators", IEE Proc., Vol. 129, Pt. C, No. 6, pp. 260-265, November 1982.

[12] Hafiz Khurshid and Narayan C. Kar*, "*Performance Analysis of Aluminum- and Copper-Rotor Induction Generators Considering Skin and Thermal Effects", IEEE Transactions on Industrial Electronics, Vol. 57, No. 1, January 2010.

[13] Miloje Kostic, "Equivalent Circuit and Induction Motor Parameters for Harmonics Studies in Power Networks", Eletrotehniski Vetstnik 79(3): pp. 135-140, 2012.

[14] Alexander Kusko and Marc T. Thompson, "Power Quality in Electrical System", The McGraw Hill, 2007.

[15] Stephen J. Chapman, "Electric Machinery Fundamentals", The McGraw Hill, 1999.

Appendix

In the saturation test, the induction machine was driven at synchronous speed by AC motor. The variable of 50 Hz voltage source is applied to the stator terminal of induction

machine for 0 to 440 Volt. For every step, the voltage applied to the stator terminal $V_t(k)$ and the current through the stator windings $I_0(k)$ are recorded. The inductance magnetizing can be solved as,

$$X_m(k) = \sqrt{\left(\frac{V_t(k)}{\sqrt{3}I_0(k)}\right)^2 - R_s^2} - X_s \text{ and } L_m(k) = \frac{X_m(k)}{2\pi f_s}$$

where: f_s is 50 Hz, and k is the test step. In this test, $I_m(k)$ is $I_0(k)$. R_s and X_s can be obtained from the results of paramater test.

Refdinal Nazir received B.E. and M.T. degree in electrical engineering from Bandung Istitute of Technology, Indonesia, in 1985 and 1991 respectively, and Ph.D degree from University Technology of Malaysia in 1999. He is currently a senior lecture in Dept. of Electrical Engineering, Andalas University, Indonesia. His research interests are electric machines, renewable energy, distributed generation, and microgrid.